

# Low-Voltage High-Transconductance Dinaphtho-[2,3-b:2',3'-f]thieno [3,2-b]thiophene (DNNT) Transistors on Polyethylene Naphthalate (PEN) Foils

Amayikai A. Ishaku, Afra Al Ruzaiqi, Helena Gleskova

Department of Electronic and Electrical Engineering, University of Strathclyde, Glasgow, UK  
ama.ishaku@strath.ac.uk

## I. SUMMARY AND MOTIVATION

Low threshold voltage, high transconductance DNNT transistors (OTFTs) with interdigitated source/drain contacts can provide low-voltage transistor amplifiers with a.c. cut-off frequency in excess of 10 kHz [1], making them suitable for wearable sensors. This paper presents an in-depth study of the geometry of such transistors fabricated on PEN. Changes in channel width-to-length ratio  $W/L$  were achieved by varying the  $W$  from  $\sim 12$  to  $\sim 18$  mm and  $L$  from 20 to 50  $\mu\text{m}$ , leading to  $W/L$  of  $\sim 300$  to  $\sim 900$ . The OTFTs exhibit threshold voltage from  $-0.33$  to  $-0.74$  V, field-effect mobility from 0.17 to 0.42  $\text{cm}^2/\text{V}\cdot\text{s}$ , on-current from 28 to 67  $\mu\text{A}$  (at  $V_{\text{GS}} = V_{\text{DS}} = -2$  V), off-current from  $6 \times 10^{-12}$  to  $7 \times 10^{-8}$  A, and subthreshold slope from 65 to 266 mV/decade. While the OTFTs exhibit large on-state drain current and a.c. transconductance, smaller  $L$  leads to a slightly reduced mobility. In addition, the OTFTs with the largest  $W$  of 18.23 mm possess the lowest off-state drain current and subthreshold slope.

## II. ADVANCES OVER PREVIOUS WORKS

The implementation of OTFTs in flexible electronics and sensors has grown exponentially in recent years. Examples include disposable sensors [2], flexible displays [3], biosensors [4] and radio frequency identification tags [5]. Traditionally, OTFTs have a 'standard' geometry where the rectangular source and drain contacts are separated by a gap. The typical  $W/L$  of 10 to 30 and the field-effect mobility of 0.5 to 1  $\text{cm}^2/\text{V}\cdot\text{s}$  lead to transistor on-current of a few microamps. Low-voltage DNNT transistors on PEN with such a standard source/drain contact geometry have shown transconductance of 12  $\mu\text{S}$  and operation up to 1 MHz. [6] The use of interdigitated source/drain contacts allows increasing the channel width of the transistor while keeping the transistor area small. As a result, the transconductance of the transistors can be further increased; making them suitable for applications where moderate switching speeds, low supply voltage and voltage gains are required. This current work reports flexible OTFTs on PEN foils (Optfine, DuPont Teijin) whose transconductance far exceeds that reported in [6], while providing the understanding of such transistor geometries.

## III. RESULTS AND METHODOLOGY

P-type OTFTs based on dinaphtho-[2,3-b:2',3'-f]thieno [3,2-b]thiophene (DNNT) were fabricated on PEN following a procedure described in [1,7]. The material and thickness of each layer from bottom to top is as follows: the gate electrode

is made of 30-nm-thick Al, gate dielectric is a bi-layer of  $\text{AlO}_x$  (13.8 nm) coated with a monolayer of octadecyl phosphonic acid ( $\text{C}_{18}\text{PA}$ , 2 nm), organic semiconductor is a 20-nm-thick DNNT and the source/drain contacts are made of 50-nm-thick Au. A top view of two OTFTs demonstrating the varying channel width, cross-sectional transistor view, and transfer characteristics are shown in Figure 1.

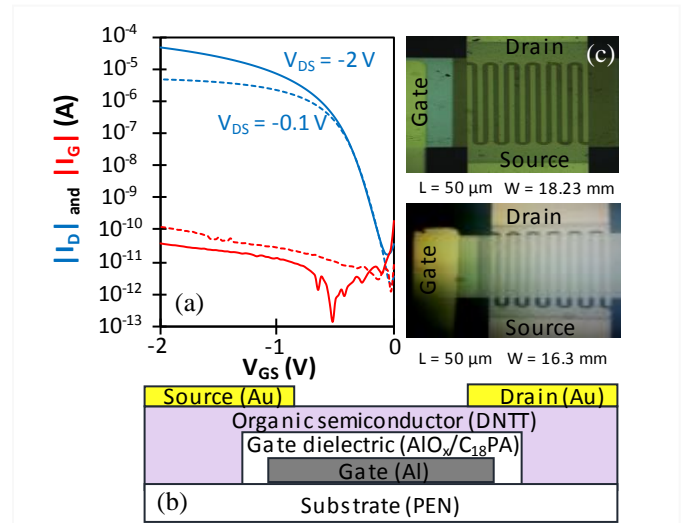


Fig. 1: Transfer characteristics for OTFT with  $L \sim 46$   $\mu\text{m}$ ,  $W = 17.12$  mm (a), cross-sectional view (b), and top views of two OTFTs with different  $W$  (c).

For the purpose of analysis, the transistors were divided into 3 groups based on their channel lengths, i.e. 20 to 30  $\mu\text{m}$ , 30 to 40  $\mu\text{m}$  and 40 to 50  $\mu\text{m}$ . The channel width was varied between 12.10 and 18.23 mm by adjusting the width of the gate electrode (see Figure 1). As a result, the  $W/L$  varied from 290 to 910. The drain current and a.c. transconductance of the transistor in saturation operation is given by Eq. (1) and (2) respectively, where  $C$  is the gate dielectric capacitance,  $\mu$  is the field-effect mobility,  $V_{\text{GS}}$  and  $V_{\text{DS}}$  are the gate-source and drain-source voltages,  $V_{\text{TH}}$  is the threshold voltage,  $I_D$  is the drain current, and  $g_m$  is the a.c. transconductance. For the a.c. transconductance measurement, a 0.2 V peak-to-peak sinusoidal wave function with a d.c. offset of  $-2$  V and frequency of 1 Hz was applied to the gate of the transistor and the drain current modulation  $I_{DPP}$  was measured.

$$I_D = \mu C \left( \frac{W}{2L} \right) (V_{\text{GS}} - V_{\text{TH}})^2 \quad (1)$$

$$g_m = \mu C \frac{W}{L} (V_{\text{GS}} - V_{\text{TH}}) = \frac{I_{DPP}}{0.2V} \quad (2)$$

Figure 2 shows the effect of  $W/L$  on the field-effect mobility, threshold voltage, on-current, off-current, and inverse subthreshold slope. At low  $W/L$ , OTFTs with the highest channel lengths ( $L = 40$  to  $50 \mu\text{m}$ ;  $W/L = 290$  to  $440$ ) display

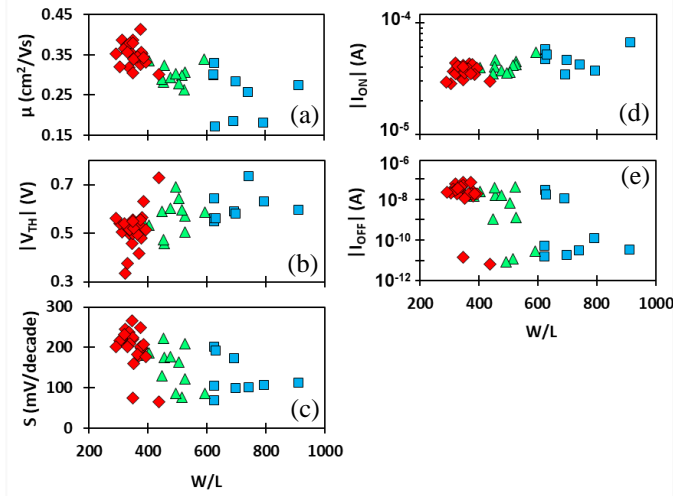


Fig. 2: Field-effect mobility (a), threshold voltage (b), subthreshold slope (c), and on- (d) and off-currents (e) as functions of  $W/L$  (legend of Fig. 3 applies).  $|I_{\text{ON}}|$  is extracted for  $V_{\text{DS}} = V_{\text{GS}} = -2 \text{ V}$ .  $|I_{\text{OFF}}| = \min(|I_{\text{D}}|)$  for  $V_{\text{GS}} = -2 \text{ V}$ .

the highest mobility of  $0.35 \pm 0.03 \text{ cm}^2/\text{V}\cdot\text{s}$ . For OTFTs with medium channel lengths ( $L = 30$  to  $40 \mu\text{m}$ ;  $W/L = 380$  to  $590$ ) the mobility reduces slightly to  $0.30 \pm 0.02 \text{ cm}^2/\text{V}\cdot\text{s}$ . Finally, OTFTs with the shortest channel lengths ( $L = 20$  to  $30 \mu\text{m}$ ,  $W/L = 620$  to  $910$ ) displayed the lowest mobility of  $0.25 \pm 0.06 \text{ cm}^2/\text{V}\cdot\text{s}$ . Figure 2(b) shows an increase in the threshold voltage from  $-0.33$  to  $-0.74 \text{ V}$  as  $W/L$  increases and channel length decreases. An average of  $-0.52 \text{ V}$ ,  $-0.57 \text{ V}$  and  $-0.60 \text{ V}$  for channel lengths of  $40$  to  $50 \mu\text{m}$ ,  $30$  to  $40 \mu\text{m}$ , and  $20$  to  $30 \mu\text{m}$  is observed, respectively. The subthreshold slope  $S$  in Figure 2(c) reduces as  $W/L$  increases and channel length decreases. OTFTs with channel lengths between  $20$  and  $30 \mu\text{m}$  exhibit subthreshold slope of  $125 \pm 48 \text{ mV}/\text{decade}$ , while transistors with  $L$  between  $30$  and  $40 \mu\text{m}$  and  $40$  to  $50 \mu\text{m}$  show values of  $147 \pm 57$  and  $198 \pm 49 \text{ mV}/\text{decade}$  respectively. The on-current of Figure 2(d) increases with rising  $W/L$ . OTFTs with  $L$  between  $20$  and  $30 \mu\text{m}$  have an average on-current of  $4.9 \times 10^{-5} \text{ A}$ ,  $L$  between  $30$  and  $40 \mu\text{m}$  leads to an average of  $4.0 \times 10^{-5} \text{ A}$  and  $L$  between  $40$  and  $50 \mu\text{m}$  to an average of  $3.9 \times 10^{-5} \text{ A}$ . Finally, Figure 2(e) shows the off-current as a function of  $W/L$ . The off-current is observed to be split into two distinct regions regardless of the channel length. This warrants further analysis that is presented next.

Figure 3(a) shows the on-current normalised with respect to the channel dimensions  $W$  and  $L$ . Based on Eq. (1) such normalised drain current should remain constant. However, the results show a gradual linear reduction in the on-state drain current as the channel length decreases and  $W/L$  increases. This reduction suggests a presence of contact resistance between the source/drain contacts and DNTT. Such contact resistance will become more dominant with decreasing  $L$ . Figure 3(b) shows the normalised off-current as a function of  $W$ . Transistors with channel widths less than  $18.23 \text{ mm}$  display an average off-state drain current of  $6.6 \times 10^{-11} \text{ A}$ . On the other hand, OTFTs with  $W = 18.23 \text{ mm}$  exhibit an average of  $3.5 \times 10^{-14} \text{ A}$ , a reduction of

$\sim 3.3$  orders of magnitude. Similarly, Figure 3(c) indicates consistently reduced subthreshold slope for OTFTs with  $W = 18.23 \text{ mm}$ , exhibiting values between  $54$  and  $114 \text{ mV}/\text{decade}$ .

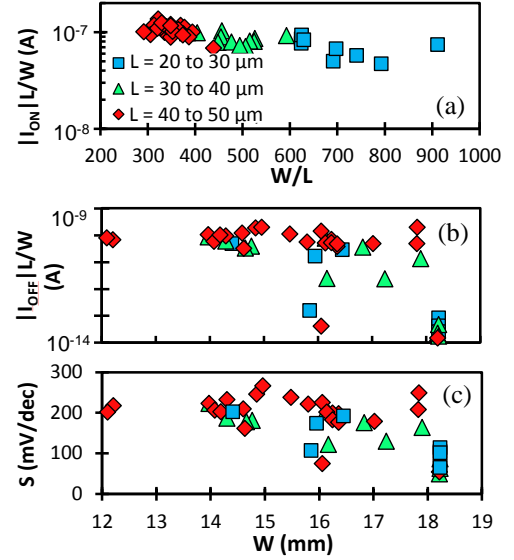


Fig. 3: Normalised transistor on-current ( $|I_{\text{ON}}| \times \frac{L}{W}$ ) versus  $W/L$  (a), normalised off-current ( $|I_{\text{OFF}}| \times \frac{L}{W}$ ) versus  $W$  (b), and subthreshold slope  $S$  versus  $W$  (c).

An example of a.c. transconductance measurement is shown in Figure 4 for three OTFTs. Drain voltage of  $-2 \text{ V}$ , source voltage of  $0 \text{ V}$  and gate voltage of  $-0.2 \text{ V}_{\text{pp}}$  ( $-2 \text{ V}$  d.c. offset) at  $1 \text{ Hz}$  were used. Transistor T1 showed the largest transconductance of  $53.2 \mu\text{S}$ , followed by T2 and T3 with  $41.3$  and  $37.9 \mu\text{S}$  respectively. The transistor cut-off frequency in excess of  $1 \text{ kHz}$  has been reported previously. [1]

In summary, optimisation of organic thin-film transistors with interdigitated source/drain contact is presented. The results confirm that the contact geometry plays an important role, predominantly affecting the off-state drain current and the subthreshold slope. The transistors with the largest  $L$  and  $W$  show the best performance.

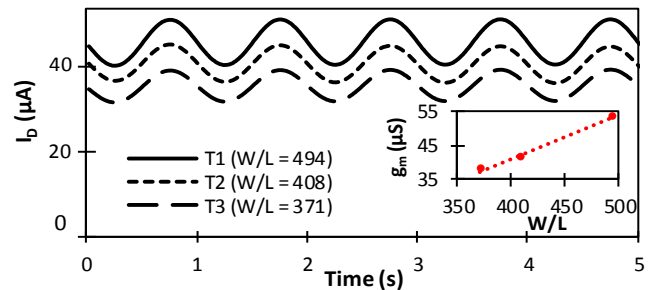


Fig. 4: A.c. drain current as a function of time ( $f = 1 \text{ Hz}$ ,  $V_G = -0.2 \text{ V}_{\text{pp}}$  with  $-2 \text{ V}$  d.c. offset,  $V_D = -2 \text{ V}$ , and  $V_S = 0 \text{ V}$ ).

#### ACKNOWLEDGMENT

This project has received funding from the European Union's Horizon 2020 research and innovation program under the Marie Skłodowska-Curie grant agreement No 734331.

## REFERENCES

- [1] Al Ruzaiqi, A., Ishaku, A. A., & Gleskova, H. (2018). Organic Thin Film Transistors With Multi-Finger Contacts as Voltage Amplifiers. *IEEE Access*, 6, 43770-43775.
- [2] Scarpa, G., Idzko, A. L., Yadav, A., Martin, E., & Thalhammer, S. (2010). Toward cheap disposable sensing devices for biological assays. *IEEE Transactions on Nanotechnology*, 9(5), 527-532.
- [3] Sheraw, C. D., Zhou, L., Huang, J. R., Gundlach, D. J., Jackson, T. N., Kane, M. G., & Francl, J. (2002). Organic thin-film transistor-driven polymer-dispersed liquid crystal displays on flexible polymeric substrates. *Applied physics letters*, 80(6), 1088-1090.
- [4] Sokolov, A. N., Roberts, M. E., & Bao, Z. (2009). Fabrication of low-cost electronic biosensors. *Materials today*, 12(9), 12-20.
- [5] Cantatore, E., Geuns, T. C., Gelinck, G. H., van Veenendaal, E., Gruijthuisen, A. F., Schrijnemakers, L., & de Leeuw, D. M. (2007). A 13.56-MHz RFID system based on organic transponders. *IEEE Journal of solid-state circuits*, 42(1), 84-92.
- [6] Zschieschang, U., Hofmockel, R., Rödel, R., Kraft, U., Kang, M. J., Takimiya, K., Zaki, T., Letzkus, F., Butschke, J., Richter, H., Burghartz, J. N., Klauk, H. (2013). Megahertz operation of flexible low-voltage organic thin-film transistors. *Org. Electron.* 14(4), 1516-1520.
- [7] Hannah, S., Cardona, J., Lamprou, D. A., Šutta, P., Baran, P., Al Ruzaiqi, A., & Gleskova, H. (2016). Interplay between vacuum-grown monolayers of alkylphosphonic acids and the performance of organic transistors based on dinaphtho[2,3-b:2',3'-f]thieno[3,2-b] thiophene. *ACS applied materials & interfaces*, 8(38), 25405-25414.